

Some physics of the two-dimensional $\mathcal{N} = (2, 2)$ supersymmetric Yang-Mills theory: Lattice Monte Carlo study

Issaku Kanamori, Hiroshi Suzuki

Theoretical Physics Laboratory, RIKEN, Wako 2-1, Saitama 351-0198, Japan

Abstract

We illustrate some physical application of a lattice formulation of the two-dimensional $\mathcal{N} = (2, 2)$ supersymmetric $SU(2)$ Yang-Mills theory with a (small) supersymmetry breaking scalar mass. Two aspects, power-like behavior of certain correlation functions (which implies the absence of the mass gap) and the static potential $V(R)$ between probe charges in the fundamental representation, are considered. For the latter, for $R \lesssim 1/g$, we observe a linear confining potential with a finite string tension. This confining behavior appears distinct from a theoretical conjecture that a probe charge in the fundamental representation is screened in two-dimensional gauge theory with an adjoint massless fermion, although the static potential for $R \gtrsim 1/g$ has to be systematically explored to conclude real asymptotic behavior in large distance.

Key words: Supersymmetry, lattice gauge theory, mass gap, screening

PACS: 11.15.Ha, 11.30.Pb, 11.10.Kk

1 Introduction

Recently, through the observation of a “partially conserved supercurrent relation”, we obtained [1] an affirmative numerical evidence that a lattice formulation in Ref. [2] provides a supersymmetric regularization of the two-

Email addresses: kanamori-i@riken.jp (Issaku Kanamori), hsuzuki@riken.jp (Hiroshi Suzuki).

dimensional $\mathcal{N} = (2, 2)$ supersymmetric Yang-Mills theory (SYM) ^{1 2}

$$S = \frac{1}{g^2} \int d^2x \operatorname{tr} \left\{ \frac{1}{2} F_{MN} F_{MN} + \Psi^T C \Gamma_M D_M \Psi + \widetilde{H}^2 \right\}, \quad (1)$$

when one supplements to S a supersymmetry breaking scalar mass term

$$S_{\text{mass}} = \frac{1}{g^2} \int d^2x \mu^2 \operatorname{tr} \{ A_2 A_2 + A_3 A_3 \}. \quad (2)$$

The scalar mass term was added to suppress a possible large amplitude of scalar fields along flat directions that may amplify $O(a)$ lattice artifacts to $O(1)$ [1]. In the present Letter, we illustrate some physical application of this lattice formulation for the system $S + S_{\text{mass}}$.

2 Correlation functions with power-like behavior

Assuming the 't Hooft anomaly matching condition, in Ref. [20], it was pointed out that the two-dimensional $\mathcal{N} = (2, 2)$ SYM has no mass gap. This aspect has been numerically investigated from almost a decade ago [21,22] by utilizing the supersymmetric discretized light-cone formulation [23]. In this super-renormalizable system, it is in fact possible to determine (to all orders of perturbation theory) an explicit form of a correlation function between Noether currents, by employing anomalous Ward-Takahashi (WT) identities (i.e. the Kac-Moody algebra) [24]; this explicit form directly proves the above assertion. Here, rather than supersymmetry, continuous global (bosonic) symmetries are important and the proof [24] applies even with supersymmetry breaking scalar mass term (2).

The total action $S + S_{\text{mass}}$ is invariant under the (two-dimensional) $U(1)_V$ transformation, $\Psi \rightarrow \exp\{i\alpha\Gamma_5\}\Psi$, and an associated Noether current ($U(1)_V$ current) is given by

$$j_\mu \equiv \frac{1}{g^2} \operatorname{tr} \left\{ \Psi^T C \Gamma_\mu \Gamma_5 \Psi \right\}. \quad (3)$$

¹ For other lattice formulations of this system, see Refs. [3–9]. For recent developments in this field of research, see Ref. [10] for a review and references cited in Ref. [1]. As further recent study, see Refs. [11–19].

² This system can be obtained by dimensionally reducing the four-dimensional $\mathcal{N} = 1$ SYM from four to two dimensions and hence a four-dimensional notation is useful; Roman indices M and N run over 0, 1, 2 and 3, while Greek indices μ and ν below run over only 0 and 1. With the dimensional reduction, it is understood that $\partial_2 = 0$ and $\partial_3 = 0$. Ψ is a four-component spinor. We follow the notational convention in Ref. [1]. Note that the gauge coupling g has the mass dimension 1.

Similarly, associated with the $U(1)_A$ symmetry, $\Psi \rightarrow \exp\{\alpha\Gamma_2\Gamma_3\}\Psi$, $A_2 \rightarrow \cos\{2\alpha\}A_2 - \sin\{2\alpha\}A_3$ and $A_3 \rightarrow \sin\{2\alpha\}A_2 + \cos\{2\alpha\}A_3$, there is a Noether current ($U(1)_A$ current),

$$j_{5\mu} \equiv \frac{1}{g^2} \text{tr} \left\{ -i\Psi^T C \Gamma_\mu \Gamma_2 \Gamma_3 \Psi + 4i(A_3 F_{\mu 2} - A_2 F_{\mu 3}) \right\}. \quad (4)$$

It is then possible to show that [24], for the two-dimensional euclidean space \mathbb{R}^2 ,

$$\begin{aligned} & -\frac{i}{2} \langle j_\mu(x) \epsilon_{\nu\rho} j_{5\rho}(0) \rangle \\ &= \frac{1}{4\pi} (N_c^2 - 1) \int \frac{d^2 p}{(2\pi)^2} e^{ipx} \left\{ -\frac{1}{p^2} (p_\mu p_\nu - \epsilon_{\mu\rho} \epsilon_{\nu\sigma} p_\rho p_\sigma) + \tilde{c} \delta_{\mu\nu} \right\} \\ &= \frac{1}{4\pi} (N_c^2 - 1) \left\{ \frac{1}{\pi} \frac{1}{(x^2)^2} (x_\mu x_\nu - \epsilon_{\mu\rho} \epsilon_{\nu\sigma} x_\rho x_\sigma) + \tilde{c} \delta_{\mu\nu} \delta^2(x) \right\}, \end{aligned} \quad (5)$$

to all orders of perturbation theory, where N_c is the number of colors and the constant \tilde{c} is a regularization ambiguity in a divergent one-loop diagram. Thus the correlation function between the $U(1)_V$ current and the $U(1)_A$ current possesses a massless pole and this is precisely what the 't Hooft anomaly matching condition claims for this two-dimensional system.

We want to confirm the power-like behavior of correlation function in Eq. (5) by using a lattice Monte Carlo simulation. For this, we prepared sets of uncorrelated configurations listed in Table 1. For simulation details, see Refs. [25,26,1]. In the table, a denotes the lattice spacing and β and L are temporal and spatial physical sizes of our lattice, respectively. The scalar mass squared is $\mu^2/g^2 = 0.25$ for all cases. The temporal boundary condition for fermionic variables is antiperiodic as in Ref. [1]. For current operator (4), we discretized the covariant derivatives $F_{\mu 2} = D_\mu A_2$ and $F_{\mu 3} = D_\mu A_3$ by using the forward covariant lattice difference. Eq. (5) suggests that we should not take an average of the correlation function over the spatial coordinate x_1 (i.e., projection to the zero spatial momentum) because after the average, correlation function (5) becomes proportional to $\delta(x_0)$ that cannot be distinguished from the regularization ambiguity; we should measure the correlation function as it stands without the zero spatial momentum projection.

In Fig. 1, we plotted $-i\langle j_\mu(x) \epsilon_{\nu\rho} j_{5\rho}(0) \rangle/2$ with $\mu = \nu = 0$ along the line $x_1 = 0$. We plotted also theoretical prediction (5) for \mathbb{R}^2 with $N_c = 2$, $(3/4\pi^2)1/(x_0)^2$, by the broken line. We clearly see the power-like fall of the correlation function for $x_0 g \lesssim 0.7$ ³ instead of exponential one, although the overall amplitude is

³ In Fig. 1, we plotted the correlation function as a function of x_0 , along the line $x_1 = 0$. As x_0 moves away from the origin $x_0 = 0$, the point x approaches a periodic image of the origin at $x_0 = \beta$ and for $x_0 \gtrsim \beta/2$ we expect the correlation function is power-like in the variable $\beta - x_0$. In other words, the fact that our

Table 1

Sets of uncorrelated configurations used for Figs. 1 and 2. The scalar mass squared is $\mu^2/g^2 = 0.25$ for all cases.

lattice size	ag	$\beta g \times Lg$	number of configurations	set label
16×8	0.1768	2.828×1.414	400	I
20×10	0.1414	2.828×1.414	800	II
24×12	0.1179	2.828×1.414	400	III
20×16	0.1414	2.828×2.263	400	IV

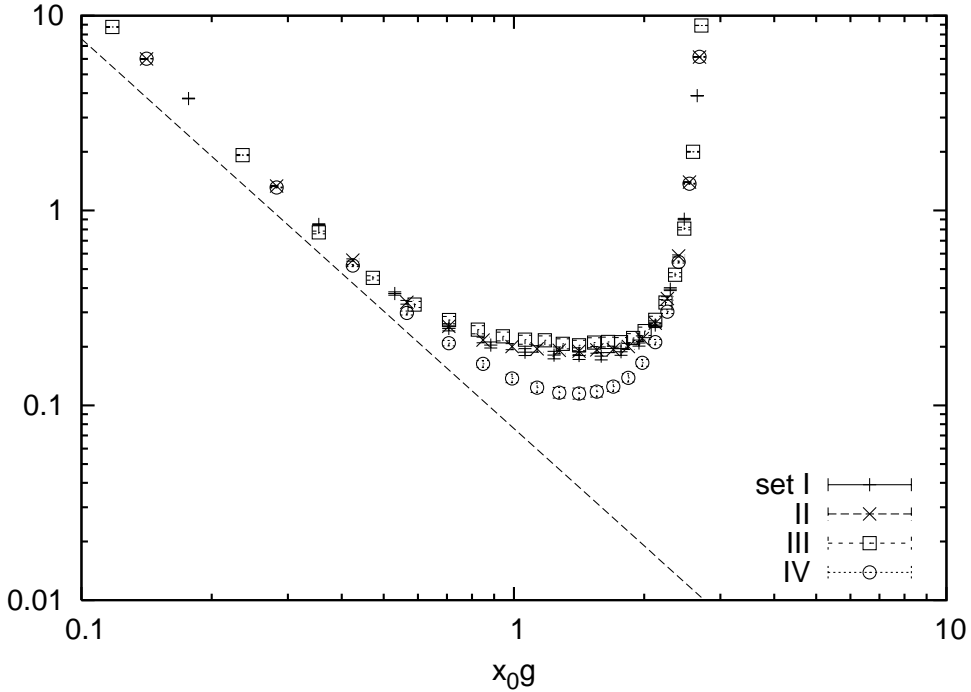


Fig. 1. The correlation function $-i\langle j_\mu(x)\epsilon_{\nu\rho}j_{5\rho}(0)\rangle/(2g^2)$ with $\mu = \nu = 0$ along the line $x_1 = 0$, for the configuration sets in Table 1. The broken line is theoretical prediction (5) for \mathbb{R}^2 .

somewhat larger than the theoretical expectation for \mathbb{R}^2 . From the behavior in the figure, we think that this discrepancy in the overall amplitude is caused by a finite lattice spacing and volume. In particular, comparison between set II (indicated by \times) and set IV (indicated by \circ) shows that the finite size effect is rather large (note that these two sets differ only in the spatial physical

finite-size lattice is topologically T^2 but not \mathbb{R}^2 cannot be neglected for $x_0 \gtrsim \beta/2$. We thus do not expect the power-like fall (that is expected for \mathbb{R}^2) for $x_0 g \gtrsim 1$ and actually the plot blows up for $x_0 g \gtrsim 1$ (in our simulation, $\beta g = 2.828$). This remark is applied also to Fig. 2, in which the antiperiodic boundary condition for fermionic fields implies “blow-down” for $x_0 g \gtrsim 1$.

size L). We thus expect that the theoretical prediction for \mathbb{R}^2 is eventually reproduced in the limit, $a \rightarrow 0$ and $\beta, L \rightarrow \infty$, although we do not carry out a systematic study on this limit.

What is the implication of the above observation? It indicates that our target theory, the two-dimensional $\mathcal{N} = (2, 2)$ $SU(2)$ SYM with a scalar mass term, is realized in the continuum limit of the present lattice model. In particular, in deriving Eq. (5), one assumes that the $U(1)_V$ and $U(1)_A$ currents j_μ and $j_{5\nu}$ individually conserve [24].⁴ One assumes $U(1)_V$ and $U(1)_A$ symmetries in this sense. In the present lattice formulation [2], the $U(1)_V$ symmetry is explicitly broken for finite lattice spacings. The above observation hence indicates that the $U(1)_V$ symmetry is fairly restored with present lattice spacings. (This symmetry will eventually be restored in the continuum limit [1].)

Now, if the system were supersymmetric, and if supersymmetry is not spontaneously broken, there would exist a massless fermionic state corresponding to the massless bosonic state appearing in Eq. (5) as an intermediate state. We expect that this fermionic state produces a massless pole in the correlation functions

$$\langle (s_\mu)_i(x)(f_\nu)_i(0) \rangle \quad (i = 1, 2, 3, 4; \text{no sum over } i), \quad (6)$$

where i denotes the spinor index and

$$s_\mu \equiv -\frac{1}{g^2} C \Gamma_M \Gamma_N \Gamma_\mu \text{tr} \{ F_{MN} \Psi \}, \quad (7)$$

$$f_\mu \equiv \frac{1}{g^2} \Gamma_\mu (\Gamma_2 \text{tr} \{ A_2 \Psi \} + \Gamma_3 \text{tr} \{ A_3 \Psi \}). \quad (8)$$

In the above, s_μ is the supercurrent associated with the supersymmetry of S , $\delta A_M = i\epsilon^T C \Gamma_M \Psi$, $\delta \Psi = \frac{i}{2} F_{MN} \Gamma_M \Gamma_N \epsilon + i \widetilde{H} \Gamma_5 \epsilon$, and $\delta \widetilde{H} = -i\epsilon^T C \Gamma_5 \Gamma_M D_M \Psi$, and f_μ is a lowest-dimensional fermionic spinor-vector (considered in Ref. [1]). Eq. (6) with $i = 1, 2, 3$, and 4 are precisely four correlation functions studied in Eq. (11) of Ref. [1] and, as noted there, these four functions are identical to each other in the continuum theory. Our expectation that Eq. (6) possesses a massless pole stems from a supersymmetric WT identity for a vanishing scalar mass squared, $\mu^2 = 0$

$$\begin{aligned} & \frac{1}{4} \sum_{i=1}^4 \langle (s_\mu)_i(x)(f_\nu)_i(0) \rangle \\ &= -\frac{i}{2} \langle j_\mu(x) \epsilon_{\nu\rho} j_{5\rho}(0) \rangle - \left\langle j_\mu(x) \epsilon_{\nu\rho} \frac{1}{g^2} \text{tr} \{ A_3(0) F_{\rho 2}(0) - A_2(0) F_{\rho 3}(0) \} \right\rangle, \quad (9) \end{aligned}$$

⁴ This assumption fails for example in the massless Schwinger model, in which the $U(1)_A$ current suffers from the axial anomaly; note that the massless Schwinger model has a mass gap.

which follows from $\delta\langle j_\mu(x)f_\nu^T(0)\rangle = 0$, where δ is the *global* super transformation; this relation holds under the assumptions that the boundary condition is consistent with supersymmetry and supersymmetry is not spontaneously broken. (In deriving Eq. (9), we have used also the equation of motion of the auxiliary field, $\widetilde{H} \equiv H - iF_{01} = 0$). In the right-hand side of Eq. (9), the massless pole in the first term (recall Eq. (5)) cannot be cancelled by the second term, because the latter is $O(g^2)$ as one can easily see.⁵

Even if the supersymmetry breaking owing to lattice regularization disappears in the continuum limit [1], our present system is not supersymmetric because there is scalar mass term (2) and we used the antiperiodic temporal boundary condition for fermions. These will give additional contribution to Eq. (9). In Fig. 2, we plotted correlation functions (6) along the line $x_1 = 0$ for set IV in Table 1. (For the parameters of this configuration set, naively-expected order of magnitude of supersymmetry breaking caused by above factors would be $\sim \mu = 0.5g$ and $\sim 1/\beta \simeq 0.3536g$, respectively.) For $0.2 \lesssim x_0g \lesssim 1.0$, for all i , the power-like behavior expected from supersymmetric WT identity (9) combined with Eq. (5) is fairly observed. Somewhat surprisingly, we do not see a significant effect of the supersymmetry breaking and it appears that the fermionic intermediate state is approximately massless as expected from approximate supersymmetry. This result is consistent with the conclusion of Ref. [1] that the supersymmetry breaking owing to the lattice regularization disappears in the continuum limit.

3 Potential energy between probe charges in the fundamental representation

Contrary to naive intuition, it is believed that a probe charge in the *fundamental* representation is screened by dynamical *adjoint* massless fermions in the two-dimensional $SU(N_c)$ QCD [27,28]. This phenomenon is analogous to the screening of a fractional charge in the massless Schwinger model with an integer-charged fermion and is believed to occur also in the two-dimensional $\mathcal{N} = (1, 1)$ SYM, despite the presence of a scalar field and a Yukawa interaction in the latter [27,29] (see also Ref. [30]). As a generalization of these, in Refs. [29,30], it was claimed that this screening persists in any two-dimensional (supersymmetric and non-supersymmetric) gauge the-

⁵ In fact, a one-loop calculation of Eq. (6) on the basis of Eq. (1) coincides with expression (5), possibly with a different regularization-dependent constant \tilde{c} . Note also that even if correlation functions (6) possess a massless pole of structure (5), this does *not* necessarily imply the existence of the Nambu-Goldstone fermion associated with the spontaneous supersymmetry breaking. This is because structure (5) shows that the Fourier transform of $\partial_\mu\langle(s_\mu)_i(x)(f_\nu)_i(0)\rangle$ vanishes at zero momentum.

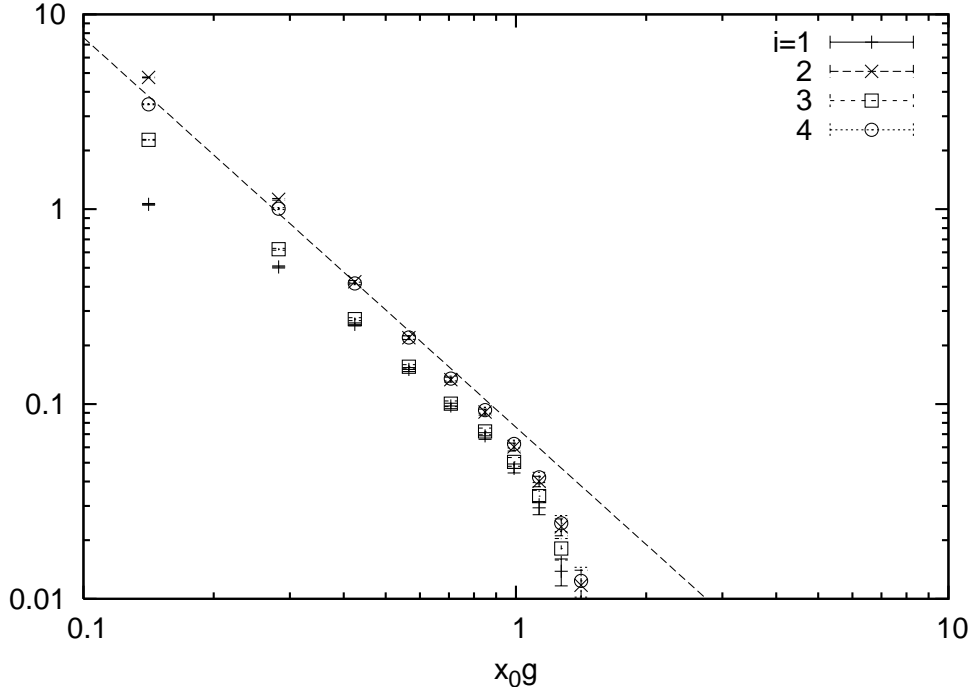


Fig. 2. The correlation function $\langle (s_\mu)_i(x)(f_\nu)_i(0) \rangle / g^2$ with $\mu = \nu = 0$ along the line $x_1 = 0$ for set IV in Table 1. The broken line is $(3/4\pi^2)1/(x_0)^2$, the same function plotted in Fig. 1.

ory with adjoint massless fermions, although an explicit proof was not given there. In our present system, the masslessness of the gaugino is ensured by the global $U(1)_A$ and $U(1)_V$ symmetries and, hence, it is of interest to study the static potential energy between probe charges in the fundamental representation. If the expected screening occurs, the static potential would approach a constant for large distance (i.e., the Wilson loop obeys the perimeter law).

We thus measure the expectation value of the Wilson loop,

$$W(T, R) \equiv \left\langle \frac{1}{2} \text{tr} \left\{ \prod_{\ell \in C} U_\ell \right\} \right\rangle, \quad (10)$$

where C denotes a rectangular loop of a physical size $T \times R$ and link variables U_ℓ belong to the fundamental representation of the gauge group $SU(2)$. For this average, we prepared uncorrelated configurations listed in Table 2 (the scalar mass squared is $\mu^2/g^2 = 0.25$ for all cases). Theoretically, the static potential $V(R)$ is defined by the asymptotic form in $T \rightarrow \infty$:

$$-\ln \{W(T, R)\} = V(R)T + c(R). \quad (11)$$

Practically, with finite-size lattices, we made a linear χ^2 -fit of $-\ln\{W(T, R)\}$ with respect to T in a finite range $T_{\min} \leq T \leq \beta/2$ for each R and regarded

Table 2

Sets of uncorrelated configurations used for Figs. 3 and 4. The scalar mass squared is $\mu^2/g^2 = 0.25$ for all cases.

lattice size	ag	$\beta g \times Lg$	number of configurations	set label
20×10	0.2	4×2	800	V
20×10	0.1414	2.828×1.414	800	VI
20×16	0.1414	2.828×2.263	400	VII
30×10	0.1414	4.243×1.414	800	VIII

the slope as $V(R)$; obviously $\beta/2$ is a maximal temporal size of the Wilson loop that is physically meaningful. We determined the lower end of the fit T_{\min} such that the fitting range becomes as wide as possible insofar as χ^2/dof of the fit does not exceed unity. We had $T_{\min} = a - 5a$. A typical result of this linear fit is depicted in Fig. 3 for the case of set VI in Table 2.

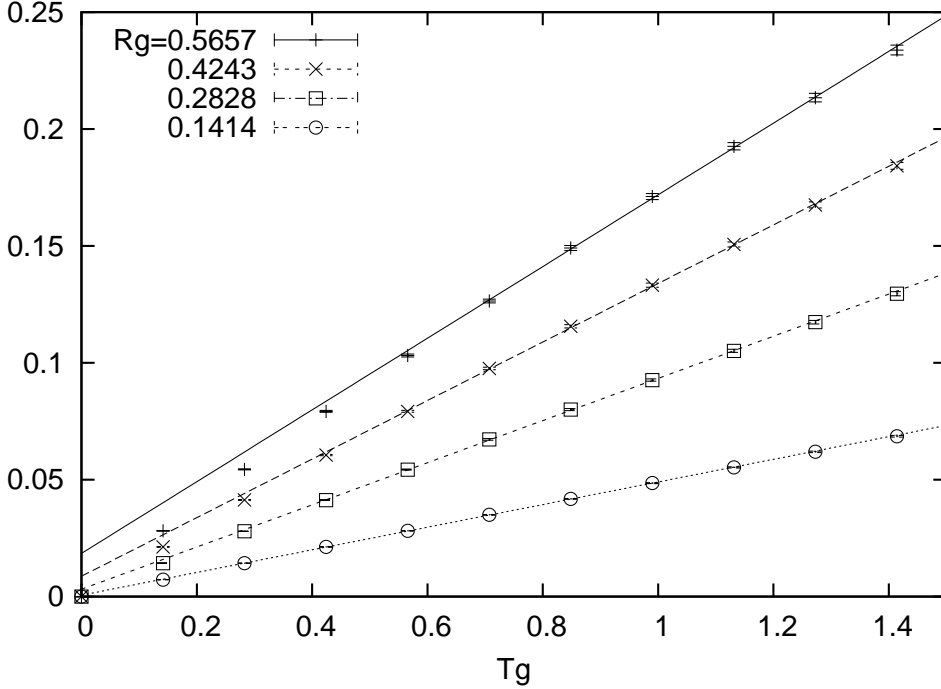


Fig. 3. The linear χ^2 -fit of $-\ln\{W(T, R)\}$ for set VI in Table 2.

In Fig. 4, we plotted $V(R)$ for $R < L/2$ determined in this way for various lattice spacings and lattice sizes (Table 2). The error in the figure was determined by the range of a slope of the linear fit that corresponds to a unit variation of χ^2 .

Now in Fig. 4, all points are almost on a common line, although lattice spacings are different ($ag = 0.2$ for $+$ and $ag = 0.1414$ for \times , \square and \circ). This fact

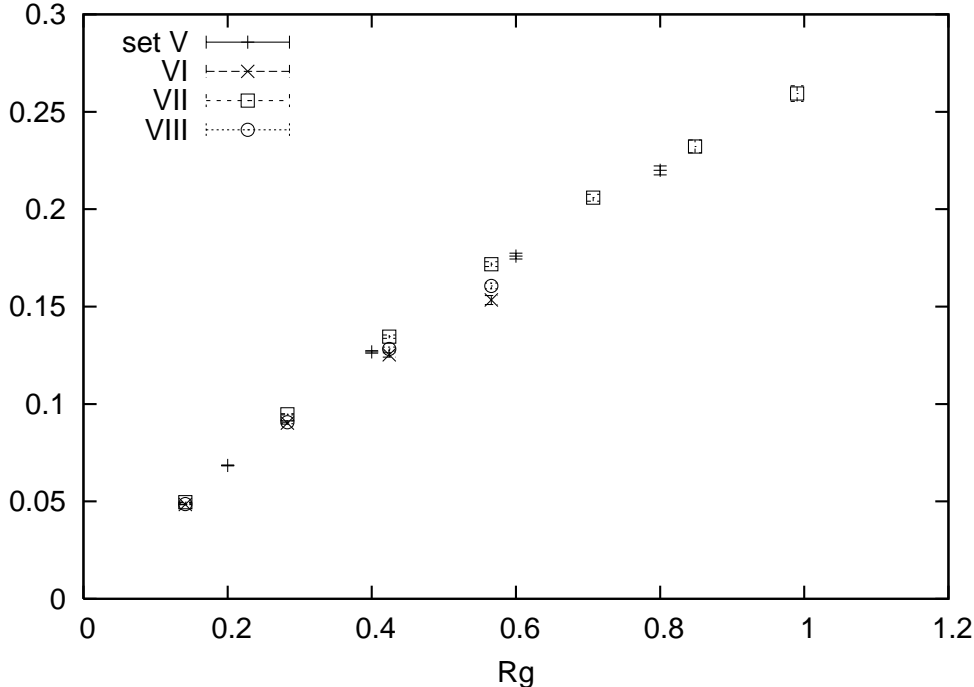


Fig. 4. $V(R)/g$ determined by the linear χ^2 -fit described in the text. See Table 2 for the label of configuration sets. $\mu^2/g^2 = 0.25$.

indicates that the result in Fig. 4 can roughly be regarded as that in the continuum limit. Similarly, since physical lattice sizes of each configuration set are rather different (for example, $Lg = 1.414$ for \times and $Lg = 2.263$ for \square), there appears almost no significant finite-size effect.⁶ Therefore, at least for $Rg \lesssim 1$, we could conclude that the static potential $V(R)$ is linear (i.e., the Coulomb potential in two dimensions) with a finite string tension $\sigma \sim 0.25g^2$. This appears to be distinct from a theoretical conjecture in Refs. [29,30].⁷ However, to conclude whether a probe charge is really confined or screened, the static potential for $Rg \gtrsim 1$ has to be systematically explored; we reserve this as a future project.

It is also of interest to see how the behavior in Fig. 4 changes as a function of the scalar mass. For example, in the limit $\mu^2/g^2 \rightarrow \infty$, the scalar fields will completely decouple⁸ and our system would become the two-dimensional

⁶ The discrepancy between \square and \times at $Rg = 0.5657$ could be explained by the fact that this value of Rg is comparable with the spatial lattice size for set VI. Note that for smaller Rg they have less discrepancies.

⁷ A possible confutation is that the gaugino is not strictly massless in our simulation because of the antiperiodic temporal boundary condition. This point seems irrelevant, however, because the behavior in Fig. 4 appears insensitive to the temporal size β of our lattice. Compare, for example, set VI and set VIII.

⁸ A unique UV divergent diagram that contains scalar loops is a one-loop scalar self-

Table 3

Sets of uncorrelated configurations used for Fig. 5.

μ^2/g^2	lattice size	ag	$\beta g \times Lg$	number of configurations
1.69	20×10	0.1414	2.828×1.1414	800
0.04	20×10	0.1414	2.828×1.1414	800

$SU(2)$ QCD with an adjoint massless fermion. On the other hand, the limit $\mu^2/g^2 \rightarrow 0$ would provide a possible definition of the two-dimensional $\mathcal{N} = (2, 2)$ SYM. It is believed that the screening occurs in both theories, as already noted. To have a rough idea on this issue, we carried out a preliminary experiment by using sets of configurations listed in Table 3. The results are summarized in Fig. 5. For both $\mu^2/g^2 = 1.69$ and $\mu^2/g^2 = 0.04$, we still see

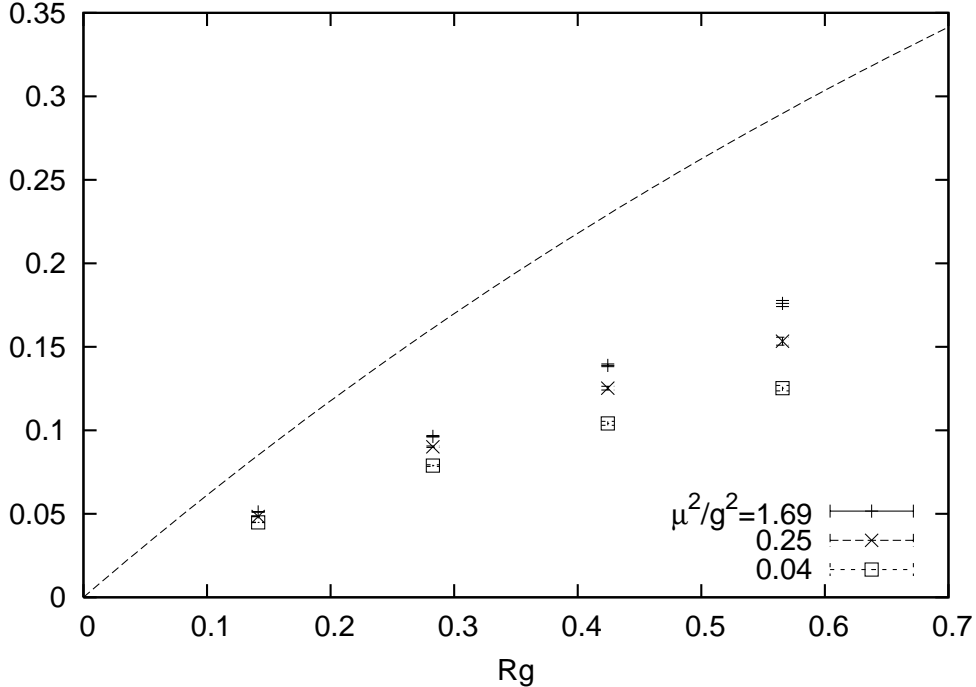


Fig. 5. $V(R)/g$ determined by linear χ^2 -fit described in the text. We used the configuration sets in Table 3 and, for $\mu^2/g^2 = 0.25$, set VI of Table 2. Eq. (12) with $N_c = 2$ is plotted by the broken line.

a linear potential, although the string tension appears somewhat smaller for

energy. This contributes to simply shift the tree-level mass μ^2 by $\sim g^2 \ln\{\mu^2/\Lambda^2\}$, where Λ is the UV cutoff, and does not affect a complete decoupling of the scalar fields in the limit $\mu^2/g^2 \rightarrow \infty$.

smaller μ^2/g^2 .⁹ In the figure, just for reference, we also plotted the function

$$V(R) = \sqrt{\frac{N_c}{\pi}} g \left(1 - \exp \left\{ -\sqrt{\frac{N_c}{\pi}} g R \right\} \right) \quad (12)$$

with $N_c = 2$, that is given by a semi-classical analysis of a bosonized version of the two-dimensional massless QCD [27]. Strictly speaking, the overall proportionality constant is not determined by this analysis and we have chosen it as above without any special reason.

Fig. 5 is simply a result with a single lattice spacing and a single lattice size. It is thus not clear what is the real behavior in the continuum and the large volume limits. Our result is still preliminary and a further detailed numerical study is needed.

4 Conclusion

In this Letter, we illustrated some numerical use of the lattice formulation [2] of the two-dimensional $\mathcal{N} = (2, 2)$ SYM with a (small) supersymmetry breaking scalar mass. Two physical problems were considered. For the first one (Sec. 2), our Monte Carlo result fairly reproduced theoretical prediction on the basis of global symmetries and (approximate) supersymmetry in the continuum theory. For the second one (Sec. 3), our result for the static potential $V(R)$ did not exhibit the screening behavior that theoretically anticipated. However, since our result of $V(R)$ was limited for $Rg \lesssim 1$, it is desirable to carry out a further systematic study by using finer and larger lattices.

We would like to thank Koji Hashimoto and Daisuke Kadoh for helpful discussions. We thank also the authors of the FermiQCD/MDP [31,32] and of a Remez algorithm code [33] for making their codes available. Our numerical results were obtained using the RIKEN Super Combined Cluster (RSCC). I. K. is supported by the Special Postdoctoral Researchers Program at RIKEN. The work of H. S. is supported in part by a Grant-in-Aid for Scientific Research, 18540305.

⁹ Consider the case $\mu^2/g^2 = 0.04$ in Fig 5. For this case, the Compton wavelength of a (free) scalar particle is $1/\mu = 5.0/g$ and this is several times longer than the physical lattice size. Thus in this case the scalar field could effectively be regarded as massless and the points \square might be regarded as those for the two-dimensional $\mathcal{N} = (2, 2)$ SYM.

References

- [1] I. Kanamori and H. Suzuki, Nucl. Phys. B **811** (2009) 420 [arXiv:0809.2856 [hep-lat]].
- [2] F. Sugino, JHEP **0403** (2004) 067 [arXiv:hep-lat/0401017].
- [3] D. B. Kaplan, E. Katz and M. Ünsal, JHEP **0305** (2003) 037 [arXiv:hep-lat/0206019].
- [4] A. G. Cohen, D. B. Kaplan, E. Katz and M. Ünsal, JHEP **0308** (2003) 024 [arXiv:hep-lat/0302017].
- [5] F. Sugino, JHEP **0401** (2004) 015 [arXiv:hep-lat/0311021].
- [6] S. Catterall, JHEP **0411** (2004) 006 [arXiv:hep-lat/0410052].
- [7] H. Suzuki and Y. Taniguchi, JHEP **0510** (2005) 082 [arXiv:hep-lat/0507019].
- [8] A. D'Adda, I. Kanamori, N. Kawamoto and K. Nagata, Phys. Lett. B **633** (2006) 645 [arXiv:hep-lat/0507029].
- [9] F. Sugino, Phys. Lett. B **635** (2006) 218 [arXiv:hep-lat/0601024].
- [10] J. Giedt, PoS **LAT2006** (2006) 008 [arXiv:hep-lat/0701006].
- [11] M. Ünsal, arXiv:0809.3216 [hep-lat].
- [12] K. Demmouche, F. Farchioni, A. Ferling, I. Montvay, G. Münster, E. E. Scholz and J. Wuilloud, arXiv:0810.0144 [hep-lat].
- [13] M. G. Endres, arXiv:0810.0431 [hep-lat].
- [14] G. Ishiki, S. W. Kim, J. Nishimura and A. Tsuchiya, arXiv:0810.2884 [hep-th].
- [15] J. Giedt, R. Brower, S. Catterall, G. T. Fleming and P. Vranas, arXiv:0810.5746 [hep-lat].
- [16] Y. Kikukawa and F. Sugino, arXiv:0811.0916 [hep-lat].
- [17] S. Catterall, JHEP **0901** (2009) 040 [arXiv:0811.1203 [hep-lat]].
- [18] K. Demmouche, F. Farchioni, A. Ferling, I. Montvay, G. Münster, E. E. Scholz and J. Wuilloud, arXiv:0811.1964 [hep-lat].
- [19] M. Hanada, A. Miwa, J. Nishimura and S. Takeuchi, arXiv:0811.2081 [hep-th].
- [20] E. Witten, Nucl. Phys. B **460** (1996) 335 [arXiv:hep-th/9510135].
- [21] F. Antonuccio, H. C. Pauli, S. Pinsky and S. Tsujimaru, Phys. Rev. D **58** (1998) 125006 [arXiv:hep-th/9808120].
- [22] M. Harada, J. R. Hiller, S. Pinsky and N. Salwen, Phys. Rev. D **70** (2004) 045015 [arXiv:hep-th/0404123].

- [23] Y. Matsumura, N. Sakai and T. Sakai, Phys. Rev. D **52** (1995) 2446 [arXiv:hep-th/9504150].
- [24] H. Fukaya, I. Kanamori, H. Suzuki, M. Hayakawa and T. Takimi, Prog. Theor. Phys. **116** (2007) 1117 [arXiv:hep-th/0609049].
- [25] I. Kanamori, PoS **LAT2008** (2008) 232 [arXiv:0809.0655 [hep-lat]].
- [26] I. Kanamori, AIP Conf. Proc. **1078** (2008) 423 [arXiv:0809.0646 [hep-lat]].
- [27] D. J. Gross, I. R. Klebanov, A. V. Matytsin and A. V. Smilga, Nucl. Phys. B **461** (1996) 109 [arXiv:hep-th/9511104].
- [28] A. Armoni, Y. Frishman and J. Sonnenschein, Phys. Rev. Lett. **80** (1998) 430 [arXiv:hep-th/9709097].
- [29] A. Armoni, Y. Frishman and J. Sonnenschein, Phys. Lett. B **449** (1999) 76 [arXiv:hep-th/9807022].
- [30] A. Armoni, Y. Frishman and J. Sonnenschein, Int. J. Mod. Phys. A **14** (1999) 2475 [arXiv:hep-th/9903153].
- [31] M. Di Pierro, Comput. Phys. Commun. **141** (2001) 98 [arXiv:hep-lat/0004007].
- [32] M. Di Pierro and J. M. Flynn, PoS **LAT2005** (2006) 104 [arXiv:hep-lat/0509058].
- [33] M. A. Clark and A. D. Kennedy, <http://www.ph.ed.ac.uk/~mike/remez>, 2005.